

Characterization of Natural Aquatic Colloids (<5 nm) by Flow-Field Flow Fractionation and Atomic Force Microscopy

M. BAALOUSHA AND J. R. LEAD*

School of Geography, Earth and Environmental Sciences,
University of Birmingham, Edgbaston,
Birmingham B15 2TT, United Kingdom

Flow-field flow fractionation (FIFFF) coupled to a UV detector and to atomic force microscopy (AFM) has been used, for the first time, to characterize ultrafine natural colloids (<5 nm) from selected freshwaters. FIFFF-UV measures a “weight diffusion coefficient distribution” and the corresponding “weight hydrodynamic diameter distribution” was calculated by applying FIFFF theory and the Stokes–Einstein equation. In addition, FIFFF has been used to prepare fractions of very narrow size range for AFM analysis. AFM measures number distribution of particle height (related to radius), and these were calculated. Both raw and transformed data show good agreement between the techniques, with conversion of the UV data to a number-weighted distribution giving better agreement and reduced errors. The small differences between the corrected data from UV analysis and the raw AFM data are either due to the fundamental differences in the analytical techniques, that is, measurement of hydrodynamic properties (FIFFF) or properties after sorption to a solid phase (AFM), or are due to the assumptions of the Stokes–Einstein equation not being met, that is, the fine natural colloids are not spherical or permeable. The methodology offers a means of quantifying fine colloid nonsphericity and permeability.

Introduction

Natural aquatic colloids are defined as solid-phase material with at least one dimension within the range 1 nm–1 μ m (1, 2). Colloids have also been defined as solid phase which presents a discrete, nonaqueous phase into which pollutants can be transported (3), although this view has been challenged in part (4). Colloids are also defined as material whose behavior is dominated by aggregation rather than sedimentation processes (5). Colloids play an important, often dominant, role in the aquatic environment in processes such as contaminant speciation, transport, and bioavailability (6–11). The importance of size in contaminant binding, and subsequent fate and behavior of trace contaminant, is well-known (12–14). Studies of the coarse colloidal fraction (>50 nm) indicated that there is an effect on trace metal partitioning because of size (and therefore assumed surface area) but that it is limited (15–18), possibly because of complex morphology of natural colloids and the presence of surface coatings. However, recent evidence has indicated that the fine fraction (<25 nm) is of prime importance in trace element partitioning (19, 20), with carbon-based carriers

of trace metals dominant at 1–4 nm and iron-based carriers dominant at 5–25 nm. The importance of the finer size fractions has been explained by increased specific surface area at smaller sizes (21). Nevertheless, there are few studies on the impact of this fine fraction on trace element speciation. Even fewer studies have been published on the structure of this fine fraction.

Nevertheless, to better understand the role of natural colloids in the environment, it is necessary to thoroughly quantify their structure and, subsequently, to determine binding mechanisms in an analogous manner to the structure–function relationship in biological macromolecules (2). This understanding is limited by the lack of nonperturbing and accurate methods to fractionate and characterize natural colloids, especially in this ultrafine region (2, 21–23), although methods such as laser-induced breakdown spectrometry (LIBD) (24), transmission electron microscopy (TEM) (25, 26), and crossflow filtration (CF) (14, 23) are becoming available. The techniques of flow-field flow fractionation (FIFFF) and atomic force microscopy (AFM) have received particular attention in recent years. FIFFF is a prominent technique for colloidal fractionation because of its excellent resolution and applicability to a wide range of sizes (27–30). FIFFF is a separation technique based on hydrodynamic principles in which particles are separated because of their interaction with the crossflow field force (friction coefficient) and their translational diffusion. For further analysis of the fractionated colloids, FIFFF has been coupled to several detectors such as UV–vis, light scattering (28, 31), graphite furnace atomic absorption spectroscopy (29, 32), inductively coupled plasma-mass spectrometry (13, 29–34), transmission electronic microscopy (31, 35), or scanning electron microscopy (36). AFM is a powerful tool for the determination of colloidal size down to the nanometric scale (25). AFM measures colloidal topography/height (*h*) on the basis of the repulsive or attractive forces between the sample and the tip, after sorption of the sample to a substrate. AFM has been previously used to image humic substances (37, 38), natural organic matter (16), natural aquatic colloids (39, 40), and freeze-dried marine water samples (26) and to examine crossflow filtration generated colloidal fractions (23). Crucially, both are capable of operating in the same nanoscale size range and are thus highly complementary.

In this study, we report the first use of FIFFF, without sample preconcentration, coupled offline with AFM. The technique was used to quantify the structure of the smallest size fraction of aquatic colloids (<5 nm), corresponding to the organic carbon-rich (possibly humic) fraction of colloids. Much of the difficulty in interpreting the results stems from the fact that FIFFF and AFM measure different weighted size distributions. FIFFF measure a weight/volume particle size distribution, while AFM measures a number particle size distribution. The objective of this work is thus to optimally couple the techniques, correctly interpret the derived information, and quantify the structure of this fine colloid fraction.

Materials and Methods

Sampling. Samples were taken from three different sites close to Birmingham, United Kingdom: Vale Lake, Bailey Brook River, and Tern River, just below the water surface. The sampling sites have been described in detail previously (40, 41). Samples were taken in winter (January and February 2006) to minimize the importance of fresh biogenic (often fibrillar) colloids. All collection bottles were high-density polyethylene and were rinsed with dilute nitric acid, pure

* Corresponding author phone: (+121) 4148147; fax: (+121) 4145528; e-mail: j.r.lead@bham.ac.uk.

TABLE 1. Summary of Samples' Physicochemical Parameters (pH and Ionic Strength), Their Number-Average Diffusion Coefficient, Number-Average Hydrodynamic Diameter Based on the VPSD Measured by FIFFF-UV, the Converted NPSD from FIFFF-UV, and the Number-Average Height Measured by AFM

fraction	pH	conductivity $\mu\text{s cm}^{-1}$	D^a ($10^{-6} \text{ cm}^2 \text{ min}^{-1}$)	d^c (nm)	D^{*b} ($10^{-6} \text{ cm}^2 \text{ min}^{-1}$)	d^{*d} (nm)	h^f (nm)	d^*/h
Vale Lake	6.5	810	2.10	2.40	2.84	1.84	1.84 (0.9–3.3) ^e	1.0
Bailey Brook	8.0	746	2.75	1.97	4.52	1.26	1.03 (0.4–5.0)	1.22
River Tern	8.0	524	3.16	1.72	4.97	1.11	0.53 (0.3–4.2)	2.10

^a D is colloidal number-average diffusion coefficient based on the FIFFF-UV VPSD. ^b D^* is colloidal number-average diffusion coefficient based on the converted FIFFF-UV NPSD. ^c d is colloidal number-average equivalent spherical diameter based on the FIFFF-UV VPSD. ^d d^* is colloidal number-average equivalent spherical diameter based on the converted FIFFF-UV NPSD. ^e Values between brackets represent the range of values. ^f h is colloid size (height) measured by AFM.

water ($R = 18.2 \text{ M}\Omega \text{ cm}^{-1}$), and the sample water, all of which were discarded. Water conductivity and pH were measured at the time of sampling and are summarized in Table 1. Samples were filtered (mixed cellulose esters, hydrophilic, $0.025 \mu\text{m}$, Millipore) in the laboratory within 2 h of sampling and were injected directly into FIFFF channel with no preconcentration. Small volumes were filtered at low flow rates, minimizing the impacts of filtration. Injection into the FIFFF was performed immediately after filtration with no storage time.

In addition to natural water samples, standard iron oxide materials have been produced and used as a standard material (small, compact, and near-spherical). The details are reported in the Supporting Information (Table SI and Figure SI). Agreement between the FIFFF and AFM measurements are excellent and are confirmed by TEM measurements.

Flow-Field Flow Fractionation. The FIFFF system used is a F1000 model Universal Fractionator (Postnova Analytics Europe, Landsberg, Germany). The channel dimensions are 29 cm in length, 2.5 cm in width, and $254 \mu\text{m}$ in thickness. A 1 kDa regenerated cellulose membrane (Postnova Analytics Europe, Landsberg, Germany) was used as the accumulation wall. Ultrapure water ($R = 18.2 \text{ M}\Omega \text{ cm}^{-1}$) with 1 mM sodium nitrate was used as a carrier solution and was degassed before delivery to the FIFFF by a PN 7505 vacuum degasser (Postnova Analytics Europe, Landsberg, Germany). The crossflow was maintained with PN1121 double piston pump and the carrier solution was delivered by a 515 HPLC isocratic pump. FIFFF fractionation conditions were 1.0 mL min^{-1} channel flow and 3.0 mL min^{-1} crossflow. A UV detector at a wavelength of 254 nm was used as a concentration detector (weight hydrodynamic diameter distribution) to determine the relative amount of the eluted particles. The fraction corresponding to the UV signal (i.e., retention volume from 1 to 3 mL) was collected after FIFFF fractionation for further analysis by AFM. Flow 2.1 software (Postnova Analytics Europe, Landsberg, Germany) was used to collect signals from the UV–vis detector. Nanospherical polystyrene polymer standards of $20 \pm 2 \text{ nm}$ hydrodynamic diameters (Duke Scientific, Palo Alto, CA) were used for the FIFFF calibration to ensure that the separation agreed with FFF theory. The standards were supplied as dispersion at a concentration of 10 g L^{-1} and were injected at 250 mg L^{-1} concentration. The channel dimensions were calculated as follows: channel thickness = $186.5 \mu\text{m}$ and channel volume = 1.03 mL.

Atomic Force Microscopy. Samples for AFM analysis were prepared applying the so-called absorption method (25), which is briefly described as follows. A freshly cleaved mica sheet surface of about 1 cm^2 was introduced into a beaker containing 3 mL of each fraction collected from FIFFF and was left for 30 min. Then, the mica sheets were withdrawn, were rinsed with ultrapure water for 30 s to remove nonadsorbed material, and were dried under ambient conditions (relative humidity 60%), in a covered Petri dish, but with an opening at the side to allow drying while preventing airborne contamination. AFM sample preparation

was performed within 12 h after sampling and AFM analysis was performed in tapping mode of a Nanoscope III instrument multimode scanning probe microscope (Digital instruments) within one week of sampling and fractionation to minimize any artifacts because of storage time. Size measurements of adsorbed colloids were performed on AFM images using the section analysis in the AFM software (40). The measured sizes were classified into intervals of 0.5-nm width to construct particle size distribution histograms (number particle size distribution). The number-average heights/hydrodynamic diameter $N(z)$ of the observed particles by AFM/eluted particles from FIFFF were determined according to eq 1 and are summarized in Table 1.

$$N(z) = \frac{\sum_i n_i z_i}{\sum_i n_i} \quad (1)$$

where n_i is the number of particles or the UV absorption and z_i is the height of each observed point by AFM or the hydrodynamic diameter measured by FIFFF.

Results and Discussion

Diffusion Coefficient and Particle Size Distribution by FIFFF. FIFFF-UV fractograms of three minimally perturbed freshwater samples (Tern River, Bailey Brook River, and Vale Lake) are presented in Figure 1. The abscissa in Figure 1a shows the retention volume (V_r) from which the diffusion coefficient (abscissa in Figure 1b) and the hydrodynamic diameter (abscissa in Figure 1c) can be calculated applying FIFFF theory (43). FIFFF-UV, which measures a weight particle size distribution, indicates that the large majority of the observed material has a hydrodynamic diameter less than 5 nm (Figure 1c). The ordinate in the three figures is proportional to the absorbance of 254-nm UV radiation. Samples show high UV absorbance in this range, which means that they have a relatively large number of chromophores which are highly active at 254 nm, and therefore, the detector sensitivity is high. At larger sizes ($> 5 \text{ nm}$), no UV signal was obtained, indicating lower absorbance of individual moieties or lower concentrations. The results indicate that in the size range $< 5 \text{ nm}$, samples are rich in UV absorbing materials, presumably natural organic matter which is humiclike in nature, in agreement with Lyven et al. (19). Number-average diffusion coefficients (D), on the basis of the weight particle size distribution from FIFFF-UV, increase in the order River Tern $>$ Bailey Brook $>$ Vale Lake (with number-average values of 3.16×10^{-6} , 2.75×10^{-6} , and $2.10 \times 10^{-6} \text{ cm}^2 \text{ min}^{-1}$, see Table 1), and their number-average hydrodynamic diameters (d) increase in the order Vale Lake $>$ Bailey Brook $>$ River Tern (number-average values of 2.4, 2.0, and 1.7 nm, see Table 1), as expected from the inverse relationship between D and d from the Stokes–Einstein relationship, which is implicit in FFF theory. Values of both size and diffusion

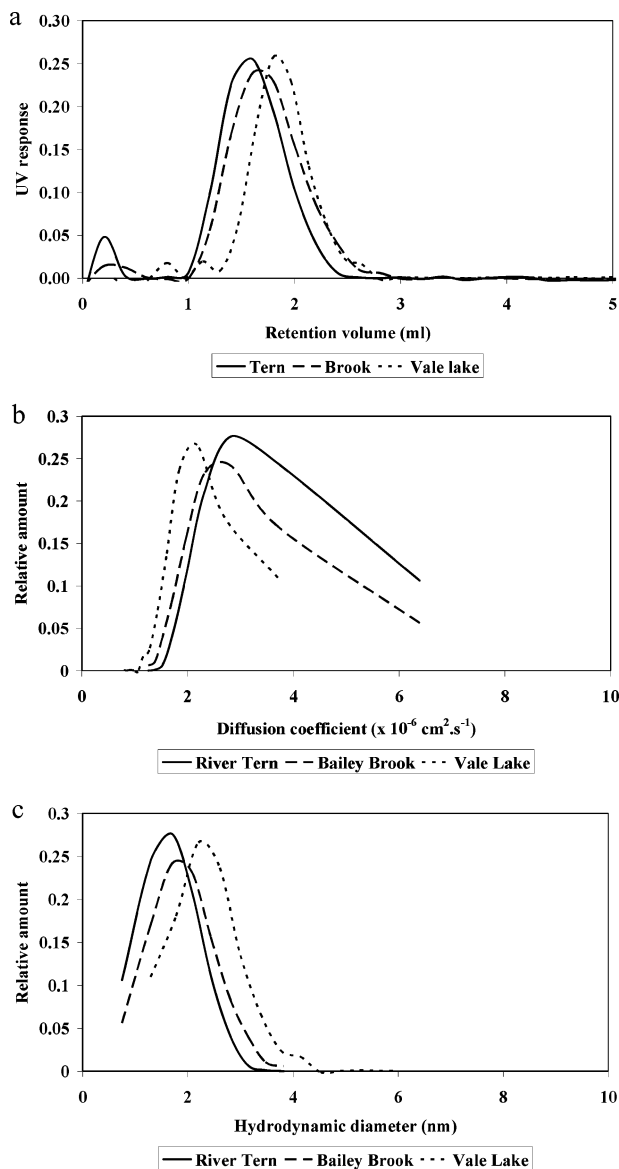


FIGURE 1. FIFFF fractograms: (a) retention volume, (b) diffusion coefficient, and (c) equivalent hydrodynamic diameter measured by FIFFF without any preconcentration. FIFFF parameters: channel flow = 1.0 mL min⁻¹, crossflow = 3.0 mL min⁻¹, channel thickness = 186.5 μm , and channel volume = 1.03 mL. UV 254 nm signal was normalized to the area under the fractograms.

coefficients are similar to those of extracted aquatic humic substances (44), again indicating that these materials are humiclike in nature.

Particle Size Distribution by AFM. Representative images of Vale Lake, Bailey Brook, and Tern colloids after sorption to a substrate (corresponding to the FIFFF-UV signal) are shown in Figure 2. Images from the Vale Lake (Figure 2a) and Bailey Brook (Figure 2b) contain mainly individual particles, while images from the Tern (Figure 2c) show single particles, often surrounded by a thin coating of less than 0.5-nm thickness, slightly resembling a “fried egg” structure. Importantly, the AFM images do not reveal any kind of association or aggregation between the fine colloidal material which confirms the limited sample perturbation expected from FIFFF and AFM when used with appropriate sample handling. AFM heights, using this preparation method (45), is ideally suited to quantify this small size fraction and so complements the FIFFF with a UV-vis detector well. The corresponding distributions of diameter, that is, height above the substrate surface, are shown in Figure 3. AFM size

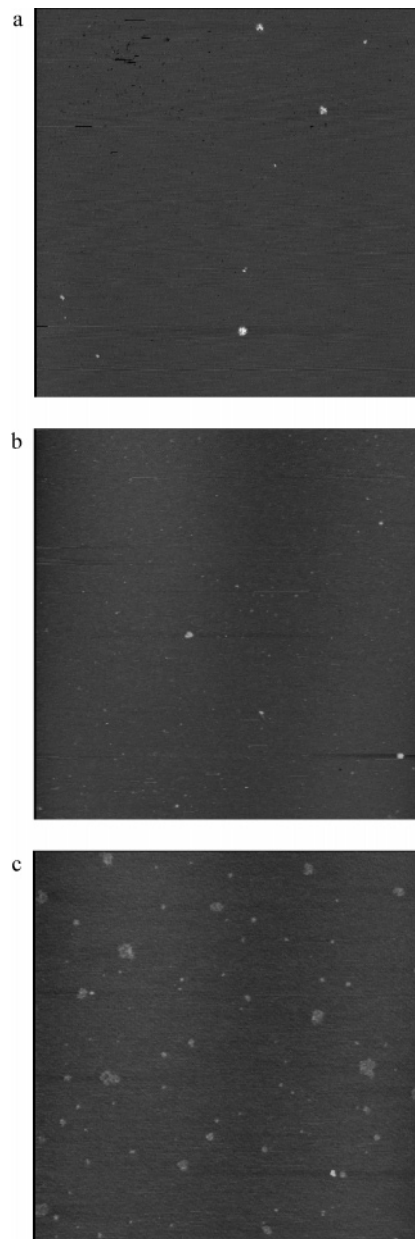


FIGURE 2. Typical AFM micrographs on the fractions collected from FIFFF without any preconcentration: (a) Vale Lake, (b) Bailey Brook River, and (c) Tern River. Image length is 5 μm .

distribution histograms (Figure 3) show a fairly homogeneous size distribution in all the samples after FIFFF separation and show that the large majority of the observed materials are less than 3.5 nm: 100% for Vale Lake, 90% for Bailey Brook River, and 98% for the Tern River. Number-average height (h), on the basis of the number particle size distribution from AFM measurements, increases in the order Vale Lake > Bailey Brook > River Tern (with number-average values of 1.84, 1.03, and 0.53 nm, respectively, see Table 1). The sizes are for the discrete particles only, not the surrounding films observed. Comparison of the directly obtained size distributions from FIFFF-UV (Figure 1) and from AFM (Figure 3) is shown in Table 1. Values of d and h are in reasonable agreement and show similar trends, that is, both the AFM and FIFFF sizes show a decreasing size from the Vale Lake, Bailey Brook, and River Tern. Thus, as a minimum, AFM supplies a size measurement independently of FIFFF and can be used to confirm FIFFF performance and to quantify any potential artifacts in FIFFF fractionation. This is especially

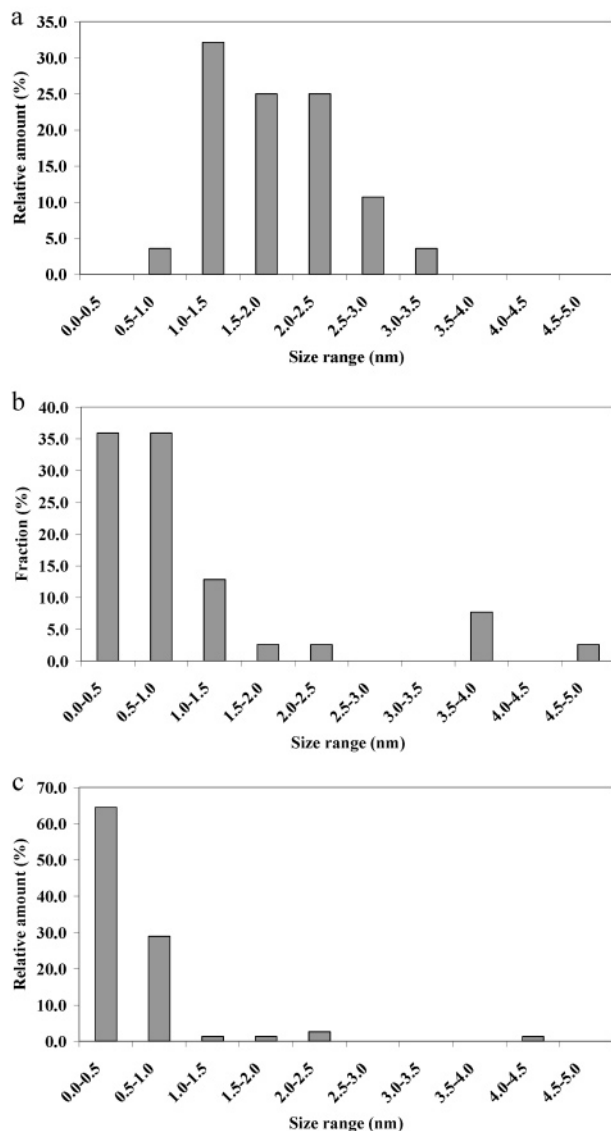


FIGURE 3. Particles size distribution on the basis of height measurement by AFM performed on the fractions collected from FIFFF without any preconcentration: (a) Vale Lake, (b) Bailey Brook River, and (c) Tern River.

useful for characterizing complex, polydisperse natural aquatic colloids.

Number versus Volume Size Distribution. Despite this reasonable agreement of the data, it is clear that the AFM results are consistently lower than the FIFFF results. In fact, the discrepancy is about a factor of 3 in the case of the River Tern (1.72 and 0.53 nm for the FIFFF and AFM, respectively). Part of this discrepancy can be explained as both AFM and FIFFF measure different size properties and therefore give a different weighted size distribution, that is, AFM produces a number-weighted distribution (number particle size distribution, NPSD) and FIFFF using a UV detector produces a weight-weighted distribution which is equivalent to volume-weighted particle size distribution (volume particle size distribution, VPSD) assuming that all the particles within this range have the same density. The NPSD and VPSD (eqs 2 and 3) should not be confused with the number-weighted average size (eq 1). NPSD and VPSD are different distributions and cannot be directly compared (*1*) without substantial errors. Thus, without further data interpretation, FIFFF and AFM might be expected to give similar but somewhat different answers, as observed. Indeed, closer inspection of Figures 1

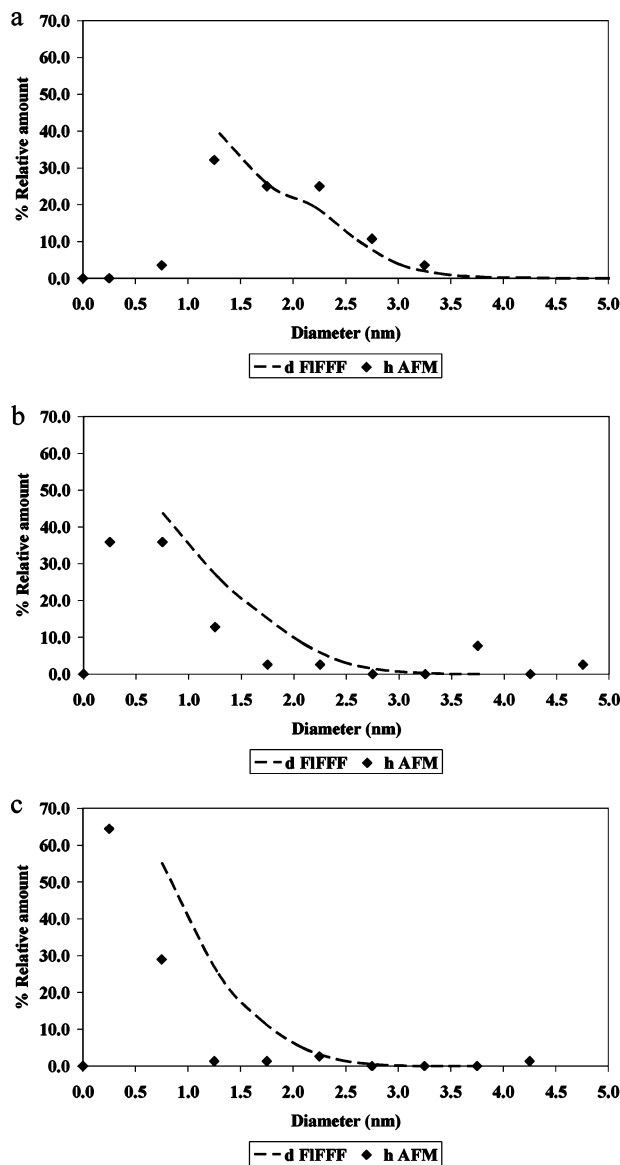


FIGURE 4. Comparison between the number particles size distribution on the basis of height measurement by AFM (data point) and the converted number particle size distribution from FIFFF (dashed line): (a) Vale Lake, (b) Bailey Brook River, and (c) Tern River.

and 3 shows differences in the size distribution (as well as their weighted means), despite the overall similarity. To compare particle size distribution measured by each technique, it is essential to convert the FIFFF VPSD to NPSD applying eq 2 or to convert the AFM NPSD to VPSD applying eq 3.

$$\% \text{ number PSD} = \left(\frac{\text{UV response}}{\text{particle volume}} / \sum \frac{\text{UV response}}{\text{particle volume}} \right) \times 100 \quad (2)$$

$$\% \text{ volume PSD} = \left(\frac{\text{particles number} \times \text{particle volume}}{\sum \text{particles number} \times \text{particle volume}} \right) \times 100 \quad (3)$$

where particle volume in eq 2 corresponds to the particle volume of each slice in the FIFFF fractogram $V = \frac{3}{4}\pi d^3$ and in eq 3 it corresponds to the midpoint interval in the AFM histogram $V = \frac{3}{4}\pi h^3$.

Conversion of the FIFFF measured VPSD to NPSD (Figure 4) shows a good agreement with the NPSD directly obtained

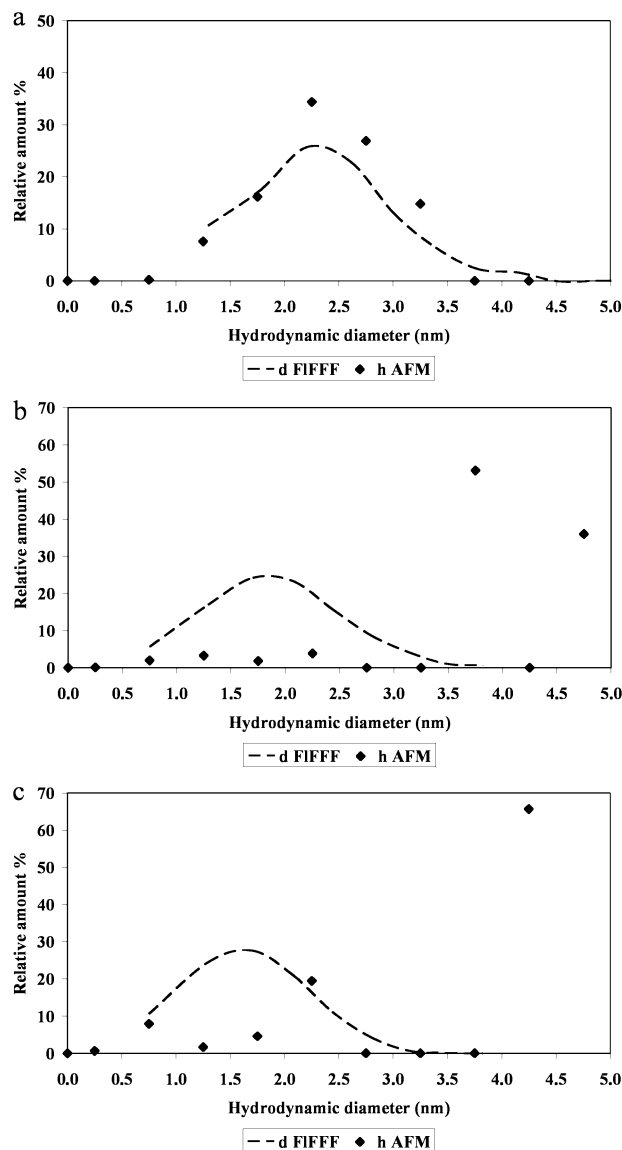


FIGURE 5. Comparison between the converted volume particles size distribution on the basis of the volume particle size distribution from FIFFF and the converted weight height from AFM measurements: (a) Vale Lake, (b) Bailey Brook River, and (c) Tern River.

by AFM in the case of the Vale Lake sample (Figure 4a). However, in the Tern River and Bailey Brook samples, AFM NPSD shows some deviations in the AFM and FIFFF PSD values, with the FIFFF data having larger proportions of the lower-sized material (Figure 4b and c). Nevertheless, the trends are generally in good agreement; number-average diffusion coefficients (D^*), on the basis of the converted FIFFF-UV number particle size distribution, increase in the order River Tern > Bailey Brook > Vale Lake (with number-average values of 4.97×10^{-6} , 4.52×10^{-6} , and 2.84×10^{-6} $\text{cm}^2 \text{min}^{-1}$, see Table 1), and their number-average hydrodynamic diameters (d^*) decrease in the order Vale Lake > Bailey Brook > River Tern (number-average values of 1.84, 1.26, and 1.11 nm, respectively, see Table 1). Converting AFM NPSD to VPSD (Figure 5) shows a fairly good agreement between AFM and FIFFF PSD in the case of Vale Lake (Figure 5a) with a higher proportion of midrange particle (2.0–2.5 nm) from AFM data. However, there is complete disagreement between AFM and FIFFF PSD for the Tern River (Figure 5b) and Bailey Brook River (Figure 5c) samples, with the larger 4–5 nm material measured by AFM absent from the FIFFF data. From Figure 5, on the basis of the converted

AFM VPSD, one might conclude that samples contain mainly large particles (>3.5 nm): 66% for the Tern River and 89% for Bailey Brook River. The results indicate that the presence of a small number of large particles > 3.5 nm will bias the whole PSD toward larger particles when converting NPSD to VPSD; a particle of 4 nm is equivalent to 64 particles of 1 nm assuming spherical geometry.

Examination of eqs 2 and 3 shows that converting VPSD to NPSD will reduce the percentage error to the third root, while converting NPSD to VPSD will increase the percentage error to the third power. This means that theoretically when comparing FIFFF and AFM size distributions, FIFFF VPSD should be converted into NPSD and not vice versa. Our results indicate that this is also the correct method of data interpretation. Thus, Figure 4 reports the most accurate interpretation of data. The conversion to a number-based distribution is most useful in interpreting aggregation phenomena (1), and it is likely that aggregation is a key process for colloids in this size range.

Interpreting the Coupled Methodology. The finding that FIFFF and AFM produce consistent results is encouraging especially given the major differences in the techniques which are based on different principles, different detection methods, and different weighted PSD (summarized in Table S1). Nevertheless, although Figure 4 data showing NPSD data are in fairly good agreement, these size distributions still do not coincide completely. Indeed, the number-average hydrodynamic diameter values shown in Table 1 again show that the number-average hydrodynamic diameter (d^*) values from FIFFF are still substantially higher than the number-average heights from the (AFM) in the case of two of the three samples. Comparison was based on Figure 4 only where AFM and FIFFF data overlap (1–5 nm). This observation might be due to two factors. First, there may simply be experimental artifacts and differences inherent in a comparison between the two techniques. Second, and more interestingly, FIFFF measures diffusion coefficient, rather than size directly, and these data must be converted to size using the Stokes–Einstein (SE) relationship. The SE relationship makes three fundamental assumptions, that the particles are small, spherical, and compact, that is, not open and penetrable by solvent or solute molecules. Deviation between the two sets of measurements might indicate that colloids are either not spherical or are permeable. The two factors are considered below.

Despite the use of appropriate AFM preparation techniques, there is no agreed method of sample preparation which will minimize sample perturbation (40). Potential artifacts in AFM include flattening of colloids after sorption to a substrate, especially where colloids are deformable and have a substantial affinity for the surface and for the occurrence of AFM tip–nanoparticle interactions, even in “tapping” mode (38–40). In addition, some hydration water essential to the structural integrity of the nanoparticle may be removed by partial air-drying (relative humidity ca. 60%). Artifacts such as these while likely to occur to some extent have not been conclusively demonstrated for aquatic colloids, although apparent underestimation of biocolloid (e.g., DNA) sizes has been observed (46). Nevertheless, further experimental development needs to be undertaken to minimize these likely problems and to include optimization of AFM preparation and analytical techniques such as the use of noncontact mode analysis in water, the use of optimum tip size and geometry, and the development of certified reference materials in the nanoscale. In addition, the FIFFF is subject to uncertainties because of aggregation from increase in nanoparticle concentration before separation or on-channel concentration (avoided in the work). These are potential problems with the methods, but changes in nanoparticle

structure, while likely, have not been demonstrated conclusively.

If these analytical uncertainties can be fully quantified, then deviation of FIFFF hydrodynamic diameter and the AFM diameter must be due to differences between the particle structure and the assumptions in the SE relationship. Thus, where the ratio of FIFFF and AFM diameter is not 1, this must be because the colloids are not spherical or are permeable (in the absence of methodological limitations). The method would thus offer an opportunity to quantify the structure of colloids relevant to environmental processes such as trace pollutant chemistry in a simple parameter which could be incorporated into, for example, speciation codes defining metal chemistry. We have performed measurements which are as accurate as possible given the analytical state-of-the-art and the problems discussed above and have found ratios (d^*/h) of 1.0, 1.22, and 2.10 for Vale Lake, Bailey Brook, and Tern, respectively. The deviations (perhaps indicating nonsphericity and permeability) agree with qualitative knowledge about nanoparticle structure. Qualitatively, the nonspherical nature of natural colloids has been demonstrated by electron and force microscopy (35, 38, 47). In addition, extracted humic substances (HS) are permeable, that is, solvent molecules and small ionic species are able to penetrate within these colloids (48, 49), although this is the first such data on nonperturbed natural colloids. Typical flow penetration lengths of 25–50% in extracted HS have been demonstrated (49) on the basis of electrophoretic mobility data. The larger ratio of d^*/h measured for the Tern sample may possibly be related to the fried egg structure observed in Figure 2c, which might result in a less spherical shape or greater permeability. The agreement in trends between d^*/h ratios and ionic strength (conductivity) suggests that variations between FIFFF and AFM measurements might be related to structural/shape variations; at the molecular level, humic substance molecules tend to become more compact with increasing ionic strength (50). Further work is obviously required. First, this trend is based on only three points and, second, suitable analytical protocols need to be developed more fully. Nevertheless, the data indicate that the derived ratios are likely to be based on structural properties to a large degree.

We have coupled FIFFF and AFM offline and have interpreted the data in a manner which will reduce experimental artifacts. The results indicate that the two techniques can be combined to usefully quantify the structure of fine aquatic colloids, although data interpretation is not simple. Initial results have provided a quantification of ultrafine colloidal structure in terms of sphericity and permeability which should have applications in modeling pollutant chemistry, fate, and behavior. Further work in developing the analytical methods and applications in nanoscience is required to have full confidence in the derived structural parameters.

Acknowledgments

This work was funded by the Natural Environment Research Council (NE/C510532/1). The authors would like to thank F. v.d.Kammer for the extensive discussion about number and volume particle size distributions and their conversions.

Supporting Information Available

Comparative data on size distributions measured on compact and roughly spherical iron oxide nanoparticles by AFM, FIFFF, and TEM are presented (Figure S1). In addition, Table S1 presents a comparison of AFM and FIFFF techniques. This material is available free of charge via the Internet at <http://pubs.acs.org>.

Literature Cited

- Lead, J. R.; Wilkinson, K. J. Environmental Colloids: current knowledge and future developments. In *Environmental Colloids: behavior, structure and characterization*; Lead, J. R., Wilkinson, K. J., Eds.; John Wiley and Sons: Chichester, UK, 2006.
- Lead, J. R.; Wilkinson, K. J. Natural aquatic colloids: current knowledge and future trends. *Environ. Chem.* **2006**, *3*, 159–171.
- Gustafsson, O.; Gschwend, P. M. Aquatic colloids: concepts, definitions and current challenges. *Limnol. Oceanogr.* **1997**, *42*, 519–528.
- Doucet, F.; Lead, J. R.; Santschi, P. H. Role of colloids in mediating trace element fate and behavior in aquatic systems. In *Environmental Colloids: behavior, structure and characterization*; Wilkinson, K. J., Lead, J. R., Eds.; John Wiley and Sons: Chichester, UK, 2006.
- Buffle, J.; Leppard, G. G. Characterization of aquatic colloids and macromolecules 1. Structure and behavior of colloidal material. *Environ. Sci. Technol.* **1995**, *29*, 2169–2175.
- McCarthy, J. F. Colloid-facilitated transport of contaminants in groundwater: mobilization of transuranic radionuclides from disposal trenches by natural organic matter. *Phys. Chem. Earth* **1998**, *23*, 171–178.
- McGechan, M. B. SW-Soil and Water: Transport of Particulate and Colloid-sorbed Contaminants through Soil, Part 2: Trapping Processes and Soil Pore Geometry. *Biosys. Eng.* **2002**, *83*, 387–395.
- McGechan, M. B.; Lewis, D. R. SW-Soil and Water: Transport of Particulate and Colloid-sorbed Contaminants through Soil, Part 1: General Principles. *Biosys. Eng.* **2002**, *83*, 255–273.
- Noell, A. L.; Thompson, J. L.; Corapcioglu, M. Y.; Triay, I. R. The role of silica colloids on facilitated cesium transport through glass bead columns and modeling. *J. Chromatogr., A* **1998**, *31*, 23–56.
- Wells, M. L.; Kozelka, P. B.; Bruland, K. W. The complexation of 'dissolved' Cu, Zn, Cd and Pb by soluble and colloidal organic matter in Narragansett Bay, RI. *Mar. Chem.* **1998**, *62*, 203–217.
- Wells, M. L.; Smith, G. J.; Bruland, K. W. The distribution of colloidal and particulate bioactive metals in Narragansett Bay, RI. *Mar. Chem.* **2000**, *71*, 143–163.
- Salim, R. Adsorption of lead on the suspended particles of river water. *Water Res.* **1983**, *17*, 423–429.
- Baalousha, M.; Motelica-Heino, M.; Babrowski, M.; Hofmeister, C.; Coustumer, P. Size based speciation of natural colloidal particles by flow field flow fractionation-inductively coupled plasma-mass spectroscopy- transmission electron microscopy/ X-energy dispersive spectroscopy: colloids-trace element interaction. *Environ. Sci. Technol.* **2006**, *40*, 2156–2162.
- Dai, M.; Martin, J. M.; Cauwet, G. The significant role of colloids in the transport and transformation of organic carbon and associated trace metals (Cd, Cu and Ni) in the Rhone delta (France). *Mar. Chem.* **1995**, *51*, 159–175.
- Taylor, H. E.; Garbarino, J. R.; Murphy, D. M.; Beckett, R. Inductively coupled plasma-mass spectrometry as an element-specific detector for field-flow fractionation particle separation. *Anal. Chem.* **1992**, *64*, 2036–2041.
- Lead, J. R.; Balnois, E.; Hosse, M.; Menghetti, R.; Wilkinson, K. Characterization of Norwegian natural organic matter: Size, diffusion coefficients, and electrophoretic mobilities. *Environ. Int.* **1999**, *25*, 245–258.
- Moon, M. H.; Kim, H. J.; Kwon, S. Y.; Lee, S. J.; Lim, H. Pinched inlet split flow thin fractionation for continuous particle fractionation: application to marine sediment for size dependent analysis of PCDD/Fs and metals. *Anal. Chem.* **2004**, *76*, 3236–3243.
- Lead, J. R.; Hamilton-Taylor, J.; Davison, W.; Harper, M. Trace metal sorption by natural particles and coarse colloids. *Geochim. Cosmochim. Acta* **1999**, *63*, 1661–1670.
- Lyven, B.; Hasselov, M.; Turner, D. R.; Haraldsson, C.; Andersson, K. Competition between iron- and carbon-based colloidal carriers for trace metals in a freshwater assessed using flow field-flow fractionation coupled to ICPMS. *Geochim. Cosmochim. Acta* **2003**, *67*, 3791–3802.
- Stolpe, B.; Hasselov, M.; Andersson, K.; Turner, D. R. High resolution ICPMS as an on-line detector for flow field-flow fractionation; multi-element determination of colloidal size distributions in a natural water sample. *Anal. Chim. Acta* **2005**, *535*, 109–121.
- Buffle, J.; Wilkinson, K.; Stoll, S.; Filella, M.; Zhang, J. A generalized description of aquatic colloids: the three colloidal component approach. *Environ. Sci. Technol.* **1998**, *32*, 2887–2899.

- (22) Filella, M.; Zhang, J.; Newman, M. E.; Buffle, J. Analytical applications of photon correlation spectroscopy for size distribution measurements of natural colloidal suspensions: capabilities and limitations. *Colloids Surf., A* **1997**, *120*, 27–46.
- (23) Doucet, F. J.; Maguire, L.; Lead, J. R. Size fractionation of aquatic colloids and particles by cross-flow filtration: analysis by scanning electron and atomic force microscopy. *Anal. Chim. Acta* **2004**, *522*, 59–71.
- (24) Bouby, M.; Geckeis, H.; Manh, T. N.; Yun, J.; Dardenne, K.; Schafer, T.; Walther, C.; Kim, J. Laser-induced breakdown detection combined with asymmetrical flow field-flow fractionation: application to iron oxide/hydroxide colloid characterization. *J. Chromatogr.* **2004**, *1040*, 97–104.
- (25) Wilkinson, K. J.; Balnois, E.; Leppard, G. G.; Buffle, J. Characteristic features of the major components of freshwater colloidal organic matter revealed by transmission electron and atomic force microscopy. *Colloids Surf., A* **1999**, *155*, 287–310.
- (26) Santschi, P. H.; Balnois, E.; Wilkinson, K. J.; Zhang, J.; Buffle, J.; Guo, L. Fibrillar polysaccharides in marine macromolecular organic matter as imaged by atomic force microscopy and transmission electron microscopy. *Limnol. Oceanogr.* **1998**, *43*, 896–908.
- (27) Beckett, R.; Jue, Z.; Giddings, C. Determination of molecular weight distribution of fulvic and humic acids using flow field-flow fractionation. *Environ. Sci. Technol.* **1987**, *21*, 289–295.
- (28) Wyatt, P. J. Submicrometer Particle Sizing by Multiangle Light Scattering following Fractionation. *J. Colloid Interface Sci.* **1998**, *197*, 9–20.
- (29) Contado, C.; Blo, G.; Fagioli, F.; Dondi, F.; Beckett, R. Characterisation of River Po particles by sedimentation field-flow fractionation coupled to GFAAS and ICP-MS. *Colloids Surf., A* **1997**, *120*, 47–59.
- (30) Hassellöv, M.; Lyvén, B.; Beckett, R. Sedimentation field-flow fractionation coupled online to inductively coupled plasma mass spectrometry—new possibilities for studies of trace metal adsorption onto natural colloids. *Environ. Sci. Technol.* **1999**, *33*, 4528–4531.
- (31) Baalousha, M.; v.d.Kammer, F.; Motelica-Heino, M.; Hilal, H.; Coustumer, P. Size fractionation and characterization of natural colloids by FIFFF-MALLS. *J. Chromatogr.* **2006**, *1104*, 272–281.
- (32) Chantiwas, R.; Beckett, R.; Jakmunee, J.; McKelvie, I. D.; Grudpan, K. Gravitational field-flow fractionation in combination with flow injection analysis or electrothermal AAS for size based iron speciation of particles. *Talanta* **2002**, *58*, 1375–1383.
- (33) Ranville, J. F.; Chittleborough, D. J.; Shanks, F.; Morrison, R. J. S.; Harris, T.; Doss, F.; Beckett, R. Development of sedimentation field-flow fractionation-inductively coupled plasma mass spectrometry for the characterization of environmental colloids. *Anal. Chim. Acta* **1999**, *381*, 315–329.
- (34) Murphy, D. M.; Garbarino, J. R.; Taylor, H. E.; Hart, B. T.; Beckett, R. Determination of size and element composition distributions of complex colloids by sedimentation field-flow fractionation-inductively coupled plasma mass spectrometry. *J. Chromatogr., A* **1993**, *642*, 459–467.
- (35) Baalousha, M.; v.d.Kammer, F.; Motelica-Heino, M.; Coustumer, P. 3D characterization of natural colloids by FIFFF-MALLS-TEM. *Anal. Bioanal. Chem.* **2005**, *308*, 549–560.
- (36) Beckett, R.; Hotchin, D. M.; Hart, B. T. Use of field-flow fractionation to study pollutant-colloid interactions. *J. Chromatogr., A* **1990**, *517*, 435–447.
- (37) Maurice, P. A.; Namjesnik-Dejanovic, K. Aggregate structures of sorbed humic substances observed in aqueous solution. *Environ. Sci. Technol.* **1999**, *33*, 1538–1541.
- (38) Balnois, E.; Wilkinson, K.; Lead, J. R.; Buffle, J. Atomic force microscopy of humic substances: Effects of pH and ionic strength. *Environ. Sci. Technol.* **1999**, *33*, 3911–3917.
- (39) Muirhead, D.; Lead, J. R. Measurement of the size and structure of natural aquatic colloids in an urbanised watershed by atomic force microscopy. *Hydrobiologia* **2003**, *464*, 65–69.
- (40) Lead, J. R.; Muirhead, D.; Gibson, C. T. Characterization of freshwater natural aquatic colloids by atomic force microscopy. *Environ. Sci. Technol.* **2005**, *39*, 6930–6936.
- (41) Cumberland, S. A.; Baker, A. The freshwater dissolved organic matter fluorescence-total organic carbon. *Hydrol. Proc.* **2006**.
- (42) Clay, A.; Bradley, C.; Gerrard, A. J.; Leng, M. J. Using stable isotopes of water to infer wetland hydrological dynamics. *Hydrol. Earth Syst. Sci.* **2004**, *8*, 1164–1173.
- (43) Giddings, J. C. Field-flow fractionation: separation and characterization of macromolecular colloidal-particulate materials. *Science* **1993**, *260*, 1456–1465.
- (44) Lead, J. R.; Wilkinson, K. J.; Balnois, E.; Cutak, B.; Larive, C.; Assemi, S.; Beckett, R. Diffusion coefficients and polydispersities of the Suwannee River fulvic acid: comparison of fluorescence correlation spectroscopy, pulsed-field gradient nuclear magnetic resonance and flow field-flow fractionation. *Environ. Sci. Technol.* **2000**, *34*, 3508–3513.
- (45) Balnois, E.; Wilkinson, K. Sample preparation techniques for the observation of environmental biopolymers by atomic force microscopy. *Colloids Surf., A* **2002**, *207*, 229–242.
- (46) Allen, M. J.; Hud, N. V.; Balooch, M.; Tench, R. J.; Siekhaus, W. J.; Balhorn, R. Tip-radius-induced artifacts in AFM images of protamine-complexed DNA fibers. *Ultramicroscopy* **1992**, *42–44*, 1095–1100.
- (47) Junta-Rosso, J. L.; Hochella, M. F.; Rimsidt, J. D. Linking microscopic and macroscopic data for heterogeneous reactions illustrated by the oxidation of manganese (II) at mineral surfaces. *Geochim. Cosmochim. Acta* **1997**, *61*, 149–159.
- (48) Warwick, P.; Hall, A.; Pashley, V.; Bryan, N. Investigation of the permeability of humic molecules using zeta potential measurements. *Chemosphere* **2001**, *45*, 303–307.
- (49) Duval, J. F. L.; Wilkinson, K. J.; van Leeuwen, H. P.; Buffle, J. Humic substances are soft and permeable: evidence from their electrophoretic mobilities. *Environ. Sci. Technol.* **2005**, *39*, 6435–6445.
- (50) Wang, Y.; Combe, C.; Clark, M. M. The effects of pH and calcium on the diffusion coefficient of humic acid. *J. Membr. Sci.* **2001**, *183*, 49–60.

Received for review July 25, 2006. Revised manuscript received November 21, 2006. Accepted November 21, 2006.

ES061766N